*Journal of the Meteorological Society of Japan*, Vol. 90B, pp. 1–10, 2012
doi:10.2151/jmsj.2012-B01 

# GCM Bias of the Western Pacific Summer Monsoon and Its Correction by Two-Way Nesting System

**Masaru INATSU, Yuya SATAKE**

*Graduate School of Science, Hokkaido University, Sapporo, Japan*

**Masahide KIMOTO**

*Atmosphere and Ocean Research Institute, The University of Tokyo, Kashiwa, Japan*

**and**

**Natsuko YASUTOMI**

*Research Institute for Humanity and Nature, Kyoto, Japan*

*(Manuscript received 16 June 2011, in final form 12 December 2011)*

**Abstract**

Accurate simulation of summertime convection associated with the Asian monsoon trough over the subtropical western Pacific is important but difficult to achieve in many general circulation models (GCMs). This study reports a case in which bias could be reduced by introducing a higher-resolution regional atmospheric model (RAM), two-way nested in an atmospheric GCM over the western Pacific. Additional partial-coupling experiments revealed that GCM bias correction was insensitive to the coupling domain. The two-way nesting effect was similar to one phase of a leading mode of natural variability in the system. This is indicative that the two-way nesting model provides more realistic tropical heating that effectively excites a correct phase of the intrinsic dynamical mode to reduce GCM bias.

## 1. Introduction

The summer monsoon in the western North Pacific is characterized by the Asian monsoon trough cutting into the western Pacific subtropical high. Along the western edge of the anticyclone, moist air is transported toward the rainband called the Baiu/Meiyu front which brings a humid climate in the East Asian summer. The interannual and intraseasonal variability of the East Asian summer monsoon has been extensively investigated. Nitta (1987) found a teleconnection pattern called the Pacific–Japan (PJ) pattern, in which a deep convection anomaly around the Philippines was linked with a barotropic vortex anomaly around Japan. The pattern is sometimes concurrent with the El Niño–Southern Oscillation (ENSO), but the precipitation difference between warm and cold events is similar to the PJ pattern (Wang et al. 2001). Differences between summers before and after the El Niño winter have also been contrasted with variability in the western Pacific climate (Wang et al. 2003; Xie et al. 2009). Most recent research has suggested that the PJ pattern can be interpreted as a dynamical mode, however. Focusing on the dominant pattern of the western Pacific summer monsoon, Yasutomi (2003) demonstrated that the pattern could be understood as a near-neutral dynamical mode using a dry linear baroclinic model (Watanabe and Kimoto 2000).

Corresponding author: Masaru Inatsu, Graduate School of Science, Hokkaido University, Rigaku bldg. 8, N10W8, Sapporo 060-0810, Japan.
E-mail: inaz@mail.sci.hokudai.ac.jp

Kosaka and Nakamura (2006) subsequently used energetics analysis to identify the PJ pattern as a moist neutral mode. Extending the discussion, Hirota and Takahashi (2011) emphasized a tripolar pressure pattern characterized by a high correlation between Baiu rainfall and deep convection around the Philippines. The pattern was found in a recently observed trend (Hirota et al. 2005) and in a global warming response (Kimoto 2005). This series of studies might lead to consensus that the leading variability in the western Pacific summer monsoon is an easily excited intrinsic dynamical mode. The leading statistical mode in the western North Pacific based on outgoing longwave radiation (OLR; Fig. 1; see section 3b for more details) actually characterizes the vortex east of the Philippines as anti-correlated with the vortex south of Alaska. When the anticyclonic (cyclonic) anomaly is located east of the Philippines, the OLR is higher (lower) there. This suggests that convection east of the Philippines is a key agent in the PJ or tripolar pattern.

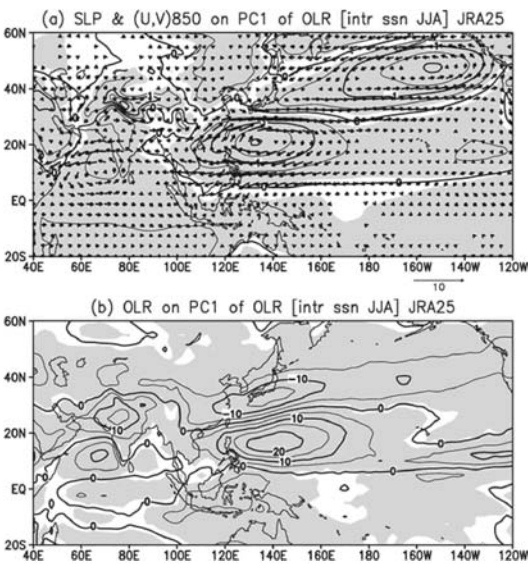


Fig. 1. (a) Sea-level-pressure (SLP; contour) and 850-hPa horizontal wind (vector) and (b) outgoing longwave radiation (OLR) regressed on the first principal component (PC) of intra-seasonal variation of OLR in 100°E–180° and 10°S–50°N for the JRA25 reanalysis data. Contour interval is 0.5 hPa and wind vector reference is at the bottom right for (a). Shading denotes statistical significance at >5% level.

On the other hand, some general circulation models (GCMs) suffer from bias over the subtropical western Pacific. Looking at the GCM climatology of Zwiers (1993), there was too much rainfall, accompanied by a low-pressure anomaly around the Philippines and a weaker jet stream in the upper troposphere. More recently, some simulations in the Fourth Assessment Report of the Intergovernmental Panel on Climate Change seem to share this bias (Lin et al. 2008). If, however, a GCM were to be combined with a regional atmospheric model (RAM), with the expectation of providing more realistic simulations, some GCM biases could possibly be corrected. This notion is encouraged by Ji and Vernekar (1997), who nested a RAM in a GCM and successfully simulated the Indian summer monsoon in both the warm and cold events of ENSO.

The conventional nesting system, however, needs a vast domain to investigate the effect of tropical diabatic heating to mid-latitude atmospheric motion. As an aside, the RAM never includes atmosphere outside of the domain, let alone intrinsic global modes like the PJ pattern. In any case, realization of a high-resolution GCM is difficult, due to heavy computational requirements. A two-way nesting climate model, coupling a GCM with an RAM, may provide a reasonable solution to examine the global response to accumulated small-scale forcing in a limited domain, thereby reducing the need for computation. Specifically, the two-way nesting model potentially realizes a GCM simulation by automatically and continuously replacing GCM forcing with forcing simulated in the RAM. Pioneering work on two-way nesting GCMs (Lorenz and Jacob 2005) successfully reduced well-known GCM bias in zonal-mean tropical air temperatures, although the reason for this reduction was not examined in depth. Chen et al. (2010) have recently used another two-way nesting system to improve simulation of the southeast China climate.

The purpose of the paper is to correct GCM bias toward low pressure and excessive deep convection in the subtropical North Pacific by using a two-way nesting climate model originally developed by Inatsu and Kimoto (2009). Coupling a GCM named the Model for Interdisciplinary Research on Climate (MIROC) with the Japan Meteorology Agency/Meteorological Research Institute (JMA/MRI) non-hydrostatic model (NHM), they found that small mountains in Northeast Asia potentially had a global effect due to modification of local circulation downstream from the mountains. Moreover, they proposed, as a condition for reduction of GCM bias by the two-way nesting system, that the RAM nested in the GCM should be able to simulate a particular phenomenon that the GCM partially or completely missed. The present study presents such a case. Since the leading dynamical mode tends to be excited in the western North Pacific in boreal summer, it is worth noting that when discussing GCM bias correction in the western Pacific boreal summer we must inevitably consider this mode. Otherwise, the problem would not produce a solution such that well-defined forcing simply excites a particular atmospheric response in the mid-latitudes. The rest of this paper is organized as follows. A model experiment and dataset are described in Section 2. Major results from sensitivity experiments while adjusting the coupling region and from comparison of the two-way nesting effect with the leading modes are presented in Section 3. Concluding remarks are given in the last section.

## 2. Methodology

The model used in this study is a two-way nesting climate model named INCL version 3.0 containing the atmospheric part of MIROC (MIROC4-AGCM; Sakamoto et al. 2011) and the RAM of the JMA/MRI NHM (Saito et al. 2006). We configured the MIROC4-AGCM, calculating the global atmosphere, with a horizontal resolution of T42 and 20 vertical sigma levels. We also configured the JMA/MRI NHM, calculating the atmosphere in a limited domain, with horizontal mesh size of 50 km and 38 vertical levels in terrain-following coordinates. The ratio between GCM and RAM is about one-fifth, following the "Big-Brother" experiments (cf., Denis et al. 2003). The INCL contains a system in which the RAM takes GCM outputs as boundary conditions and returns the aggregation of the finer-mesh RAM result to the GCM within the nested area every 1 hour, which is just 3 GCM time steps. In interactive mode, GCM time increments are modified as a 50/50 mixing of GCM and RAM time increments inside the nesting domain, and the weighting function is smoothly connected to the no-mixing zone out of the border of the nesting domain (Fig. 2). Some sensitivity experiments had a smaller area of feedback from the RAM to the GCM. Other points that are not discussed above are largely the same

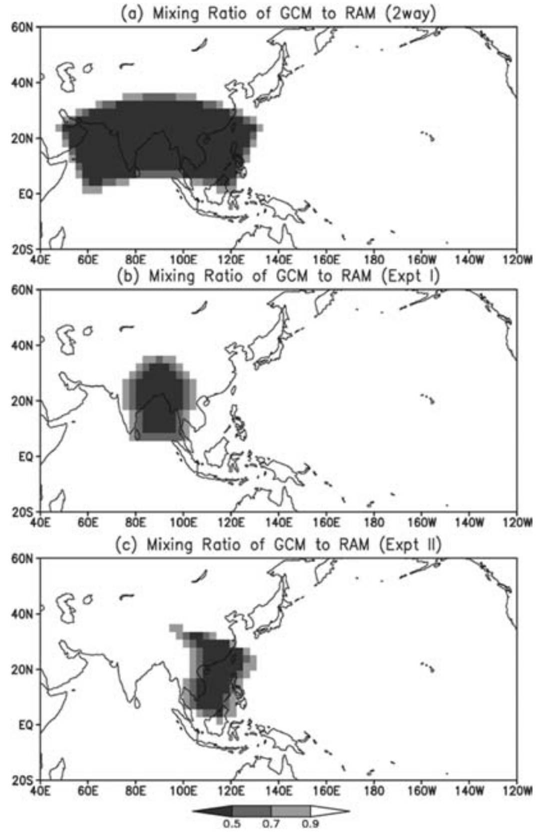


Fig. 2. The mixing ratio of the general circulation model (GCM) to the regional atmospheric model (RAM) common prognostic variables in the interactive mode experiments in INCL: (a) two-way standard experiment, (b) Experiment I, and (c) Experiment II. Gray shading as per the reference at the bottom.

as the old version of INCL used by Inatsu and Kimoto (2009). The nested domain (Fig. 3) covers the Asian monsoonal region with the Himalayas and the Maritime Continent, both of which are quite important in global climate dynamics. Monthly sea surface temperatures (SSTs) interpolated to the daily interval are given in both GCM and RAM as in Fig. 3a [see Hurrell et al. (2008) for details related to Atmospheric Model Inter-comparison Project (AMIP) SST data compilation]. Note that warm SSTs prevailed from the Indian Ocean to the tropical eastern Pacific in 1997 summer.

We performed AMIP-type integrations from 15 May 1997 to 11 October 1997, using the offline-mode and interactive-mode INCL. There were 5 ensemble members starting with different initial

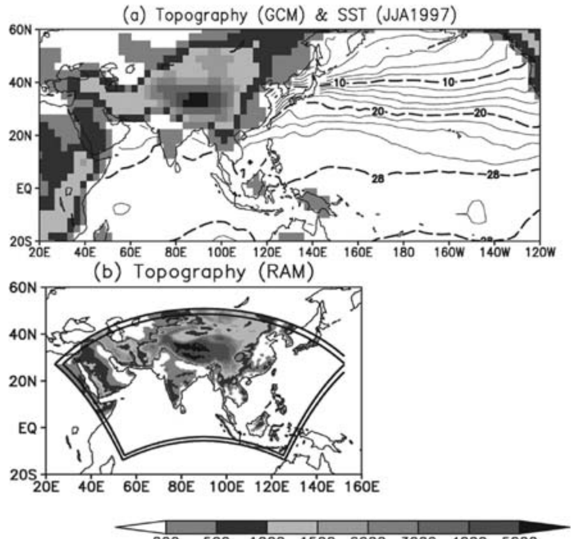


Fig. 3. (a) The surface height for the GCM (grayscale values as per the bottom reference) and sea surface temperatures (SSTs) averaged in June, July, and August (JJA) in 1997 (contour interval is 2 K and contours for 10, 20, and 28°C are indicated by thick dashed lines). (b) The surface height for the RAM (grayscale values) with the buffer zone between outer and inner thick lines.

conditions created from a control MIROC4-AGCM experiment. We took the atmospheric data on 15 May of a particular year in the experiment as the initial condition. Two sensitivity experiments, both also having five ensemble members, were designed to reveal whether GCM bias correction is independent of the region where the GCM is coupled with the RAM. Setting the same RAM domain as the standard two-way nesting integration, Experiment I connects GCM and RAM only in the Himalayas and the Bay of Bengal (Fig. 2b), and Experiment II connects the models only in the tropical western Pacific (Fig. 2c). The connecting domain in Experiment I (II) is only the middle (eastern) one-third of the RAM domain. The dry linear primitive equation model, a derivative of MIROC, was used to diagnose the two-way nesting effect, following the idea of Yasutomi (2003). See Watanabe and Kimoto (2000) for the model description and section 3c for how to use the model.

The dataset for estimating model biases is 6-hourly Japanese Meteorological Agency reanalysis data named JRA25 (Onogi et al. 2007) of which horizontal mesh is $1.25^\circ \times 1.25^\circ$ and National Atmosphere and Ocean Administration (NOAA) interpolated OLR data (Liebmann and Smith 1996).

## 3. Results

### *3.1 GCM bias correction*

Figure 4 illustrates the Asian summer monsoon in 1997, both by observation and the GCM simulation. Without any caveat the GCM result denotes the ensemble mean of results in the GCM experiment. Reviewing the summer monsoon (Fig. 4a), there was a strong clockwise vortex in the North Pacific with its center of action at 150°E and 35°N, and another clockwise vortex in the equatorial Indian Ocean. The deep convection accompanied by the tropical low pressure was located in western India, in the Bay of Bengal, and around the Philippines. Even in the pre-El Niño summer, the western edge of the summer subtropical anticyclone reached the coast of China. For the most part, the GCM simulation (Fig. 4b) captured the structure of the Asian summer monsoon. However, it overemphasized the contrast between the monsoon trough and subtropical anticyclone, with a noticeable bias of the intrusion of the monsoon trough toward the western North Pacific, accompanied by a low OLR region prevailing around 170°E and 20°N (Fig. 4c). This bias potentially distorts the climate of Northeast Asia, because it is located at a key region for dominant variability in the western North Pacific. Some conventional GCMs suffered from the bias, as was mentioned in the Introduction.

Figure 5 shows the ensemble mean of results in the two-way nesting GCM, hereafter referred to as the INCL results. The GCM-RAM coupling better simulated the subtropical anticyclone. Also corrected were the excessive intrusion of the monsoonal low toward the Philippines, and the fictitious active convection in the subtropical North Pacific (Figs. 4b,c). The two-way nesting system therefore successfully reduced the bias in the western North Pacific in summer 1997, although the inland low pressure and Indian monsoonal wind were still too strong (Figs. 4c, 5b).

Figures 6a,b show the difference between INCL and GCM results, that is, the impact of the interactive nesting. The interactive nesting provided a high pressure anomaly south of Japan and a low-pressure anomaly northeast of Japan, both statistically significant at $>95\%$ confidence level. The nesting also made the OLR higher in the subtropical North Pacific and lower along the Baiu/Meiyu

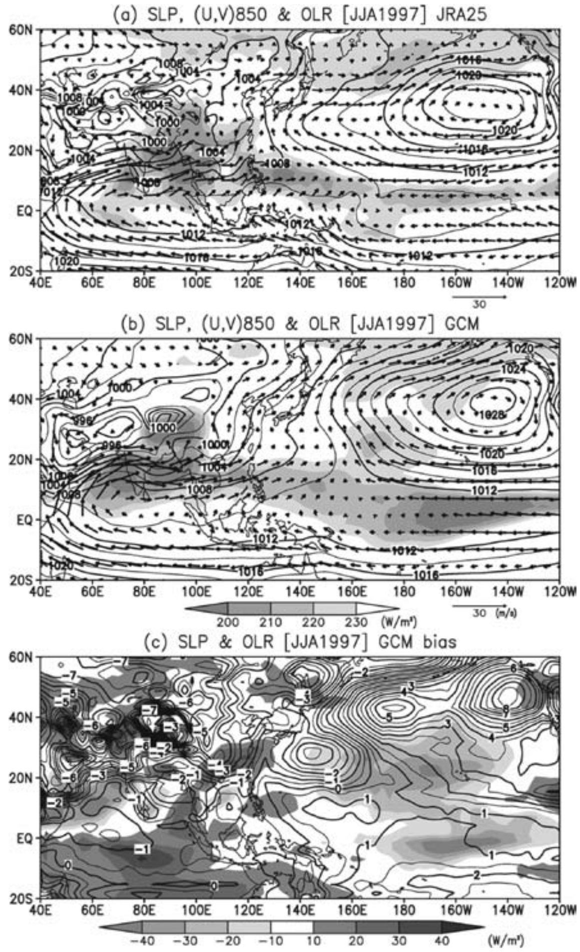


Fig. 4. SLP (contour), 850-hPa horizontal wind (vector), and OLR (shading) averaged in JJA 1997 (a) for the Japanese JRA25 reanalysis data and (b) for the ensemble-mean of the Atmospheric Model Inter-comparison Project (AMIP)-type simulation using an uncoupled GCM experiment. Contour interval is 2 hPa, thick labeled every 4 hPa; a vector reference is shown in the bottom right, and a shading reference is shown in the bottom of (b). (c) GCM bias for SLP and OLR, with contour interval 0.5 hPa and shadings as per the bottom reference.

front in Northeast Asia. Setting the coupling region in the middle one-third of the nesting domain in Experiment I (Fig. 6c), the interactive nesting impact is quite similar to the full coupling though with less statistical significance in the low-pressure anomaly. Moreover, setting the coupling domain

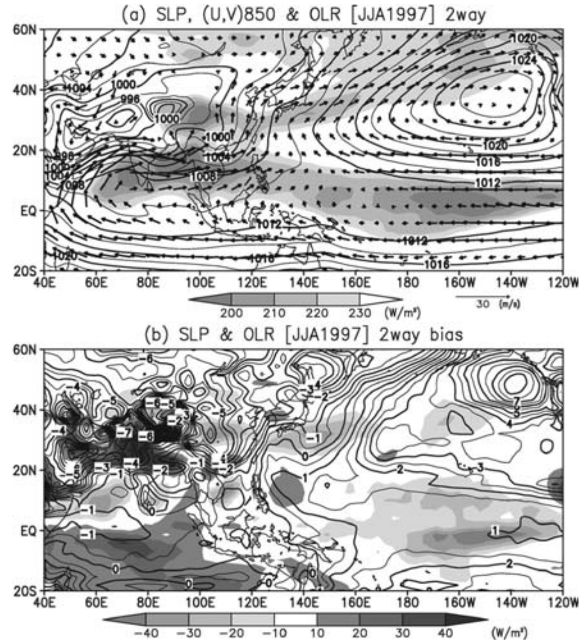


Fig. 5. Same as Figs. 4b,c, but for the two-way nesting GCM.

in the eastern one-third in Experiment II (Fig. 6d), the interactive nesting impact weakened but Japan was still sandwiched between the high- and low-pressure anomalies, as in the full coupling. These results suggest an intrinsic dynamical mode being excited by the two-way nesting impact, although the interactive nesting impact (Fig. 6) is slightly shifted eastward as compared with the observed dynamical mode pointed out in many earlier studies (Hirota and Takahashi 2011; Kosaka et al. 2009; Yasutomi 2003).

### *3.2 Leading statistical modes*

As anticipated from the discussion in the Introduction, two-way-nesting successfully corrected the western North Pacific bias from which some GCMs suffer, and results were not sensitive to the domain size where the GCM collected RAM information. The mechanism by which the INCL reduces GCM bias is likely excitation of a leading dynamical mode inherent in the western North Pacific. In this subsection, we will compare the INCL results with the leading statistical mode in the GCM.

Figure 7 shows the regression map onto the first principal component (PC) of intra-seasonal variability of OLR, simulated by the uncoupled GCM during the JJA 1997 experiment. To calculate the PCs, we first archived the pentad-mean OLR data

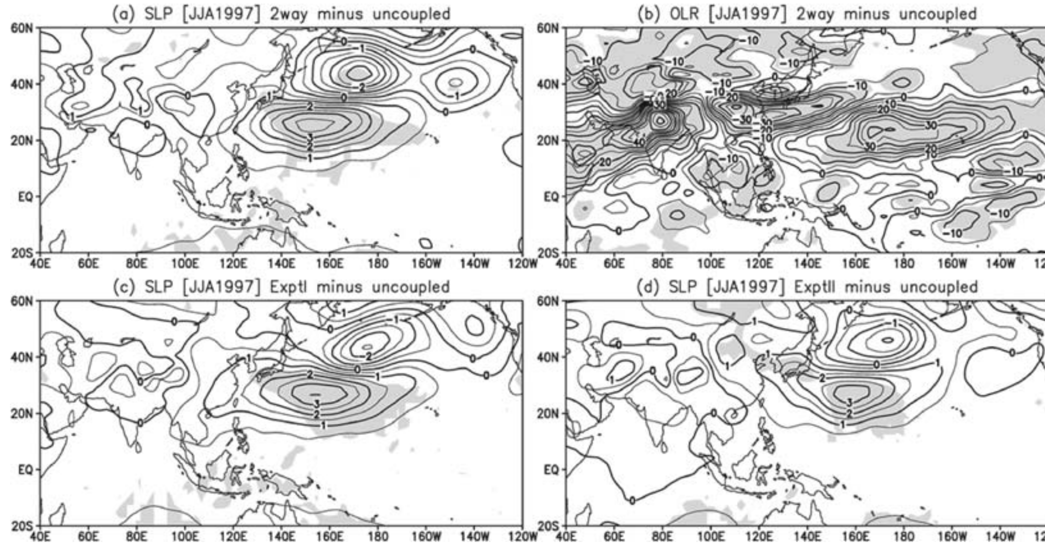


Fig. 6. SLP difference between two-way nesting GCM and uncoupled GCM in JJA 1997. Contour interval is 0.5 hPa with thick labels every 1 hPa. Shading denotes statistical significance at >5% level. (b) Same as (a), but OLR with contour interval 5 W m$^{-2}$. (c,d) Same as (a), but for (c) difference from Experiment I and (d) difference from Experiment II.

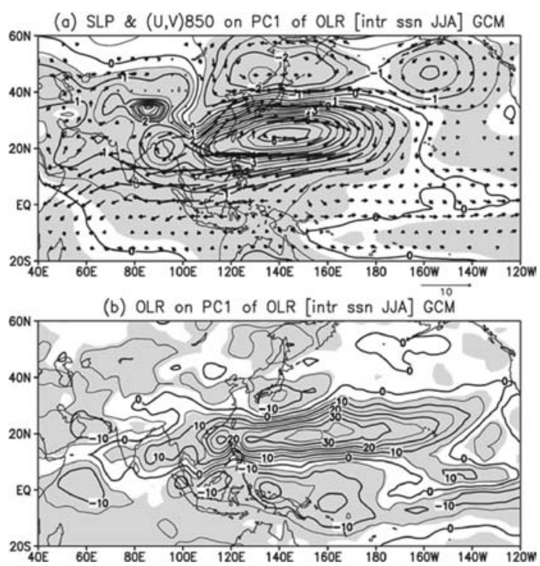


Fig. 7. (a) SLP (contour) and 850-hPa horizontal wind (vector) and (b) OLR regressed on the first principal component (PC) of intra-seasonal variation of OLR in 100°E–180° and 10°S–50°N for all ensemble members of the uncoupled GCM simulation. Contour interval is 0.5 hPa and wind vector reference is at the bottom right for (a). Shading denotes statistical significance at >5% level.

in 100°E–180° and 10°S–50°N for every ensemble of the uncoupled GCM experiments from 1 June to 31 August, and next solved the eigenvalue problem of the covariance matrix for all the ensemble data. This method in principle included both seasonal and intra-seasonal variability in the PC time series. The seasonal trend is quite weak in all ensemble time sequences of the first PC during JJA 1997 (Fig. 8a), while it significantly projected onto the third PC (not shown). Moreover the first mode explains more than 30% of the total variance (Fig. 8b), with a clear separation from the higher modes by testing following Navarra (1993). The spatial pattern (Fig. 7) shows that the mode had a large SLP variation south of Japan, anti-correlated with a weak SLP signal in the extratropical Pacific. As for the circulation anomaly, the convection is suppressed (enhanced) in the subtropical Pacific when the anticyclonic (cyclonic) circulation is dominated there.

Comparing two-way nesting impact (Figs. 6a,b) with the uncoupled GCM's leading statistical mode (Fig. 7), there is much similarity between them. The most important features are the anticyclonic circulation south of Japan and the suppression of convection in the subtropical North Pacific. Note that the opposite sign could have appeared as the leading mode with the same probabil-

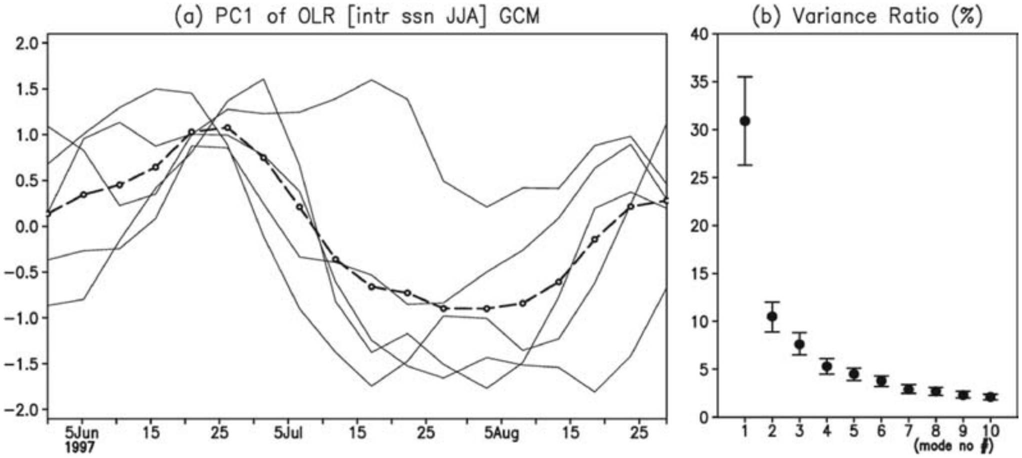


Fig. 8. The first PC of intra-seasonal variation of OLR in 100°E–180° and 10°S–50°N for JJA 1997 in the uncoupled GCM simulation. Thin solid lines denote normalized PCs for each ensemble run and the heavy dashed line denotes the ensemble average. (b) Variance ratio (%) of each PC mode to the total variance. The $x$-axis denotes the number of modes and error bars estimated following North et al. (1982).

ity. The enhancement of convection in Northeast Asia seems to be symbiotic with suppressed convection in the subtropical North Pacific, and this is more strongly emphasized in the two-way nesting impact. The cyclonic circulation in the extratropical North Pacific is a clear signal of two-way nesting impact, while it is slightly shifted westward in the observed mode. The discrepancy between leading mode and two-way nesting impact was found in OLRs in the Indian Ocean, simply because the PC analysis was performed in the region east of 100°E. The similarity between the leading statistical mode and two-way nesting impact is suggestive of the excitation of a near-neutral mode, as mentioned in the Introduction.

We remarked on the difference between the uncoupled GCM leading mode and the observed one. Looking at a regression map onto the first PC of the NOAA OLR from 1980 to 1999 (Fig. 1), the uncoupled GCM leading mode is similar to the observed one, while it much more strongly emphasized the signal in the subtropical North Pacific. The slight difference of the leading mode between the observation and the uncoupled GCM run is probably due to differences in the basic state (not shown).

### *3.3 Leading dynamical modes*

As described in the Introduction, the dominant variability in the East Asian summer monsoon can be interpreted as a moist neutral mode easily excited in the dynamical system (Hirota and Takahashi 2011; Kosaka et al. 2009). Consider a linear dynamical system and decompose its linear operator as $L = U\Sigma V^T$, following Navarra (1993). The response $x$ to a prescribed forcing $f$ is then written as $x = \sum_k \frac{(u_k, f)}{\sigma_k} v_k$, so that the response depends on both the projection of the forcing to the left singular vector (SV) $u_k$ and the magnitude of the singular value $\sigma_k$. Assuming that the two-way nesting impact is similar to one phase of the right SV for the gravest mode $m$, $v_m$, in principal one could calculate the corresponding forcing of $u_m$. However, the effective forcing pattern of the atmosphere is difficult to identify definitely, because the vector $u_m$ is formally derived from higher derivatives of $v_m$.

Here, we used a simple method to calculate the leading dynamical modes in the western North Pacific, using the dry linear primitive equation model for the uncoupled GCM result (Watanabe and Kimoto 2000). We first prepared the linear operator for the JJA-mean basic state of the uncoupled GCM result, and next calculated the left SVs estimated by the leading statistical modes of every response to temperature forcing at a single grid point over the domain of 60°E–180° and 10°N–30°N (cf. Watanabe and Kimoto 2000). The temperature forcing was prescribed by mimicking observed tropical diabatic heating with the forcing at the mid-troposphere of $5.0 \times 10^{-5}$ K s$^{-1}$ (Fig. 9a). Forcing was embedded on 330 grid points, noting that the

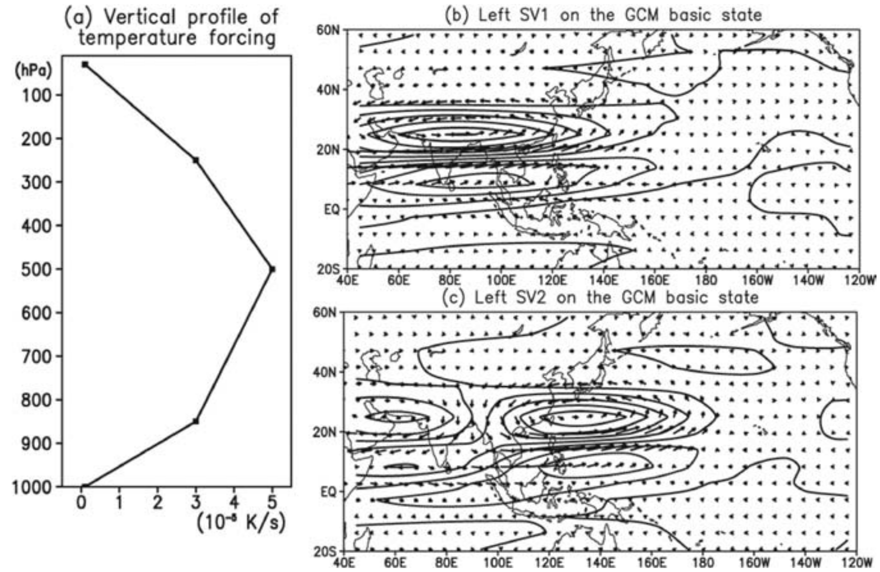


Fig. 9. (a) The vertical profile of the single-gridpoint temperature forcing in the singular vector (SV) calculation ($10^{-5}$ K $s^{-1}$) based on the uncoupled GCM background. (b) Horizontal wind vector at 850 hPa and its horizontal rotation as components of the first SV estimated as the first empirical orthogonal functions (EOFs) for every response to single-gridpoint temperature forcing scattered over 60°E–180° and 10°N–30°N. (c) Same as (b), but for the second left SV.

grid system was reduced to T21 in the linear model calculation.

Figures 9b,c show the first and second SVs on the uncoupled GCM basic state. Note that we are not able to draw the SLP picture for the SV modes, because the SLP is not a component of the response vector in the linear model. The first and second modes explain 15.9% and 14.6% of the total variance, respectively, and they do not separate from each other but rather from the higher modes (North et al. 1982). The first SV (Fig. 9b) contains a large vortex prevailing over South Asia, while the second SV (Fig. 9c) is characterized by a smaller vortex in the western North Pacific. The second SV (Fig. 9c) is similar to the leading statistical mode (Fig. 7a), although the extratropical signals are quite weak in the SV mode. The first SV (Fig. 9b) is partially similar to the second empirical orthogonal function (EOF) mode (not shown). This suggests that the uncoupled GCM leading variability found in the western North Pacific is in fact one of the dynamical modes, while the other modes with a larger-scale circulation over South Asia are comparably dominant. Moreover, an opposite phase of the second SV (Fig. 9c) is similar to the two-way nesting impact. This demonstrates that the INCL improved the regional tropical diabatic heating that excited one phase of the second SV in the western North Pacific to successfully correct the GCM bias. Further analysis could reveal how heating around the western North Pacific could effectively excite the second SV, but this is beyond the scope of this paper.

## 4. Concluding remarks

We have tried to improve GCM bias in the western Pacific summer monsoon by using a two-way nesting system in which the RAM is nested in the GCM and both models are simultaneously integrated with continuous communication between them. The two-way nesting GCM has successfully improved the excessive intrusion of the monsoon trough into the Pacific and the fictitious convection in the subtropical North Pacific, both of which some GCMs have commonly suffered from. Additional partial-coupling experiments revealed that the GCM bias correction was insensitive to the domain where GCM coupled with RAM in the two-way nesting system. On the other hand, a leading statistical mode was characterized by the two opposite-signed vortex pairs north and south of Japan. A leading SV pattern simply estimated by using a linear dynamical model more strongly emphasized the vortex south of Japan. These statistical and dynamical patterns were actually similar to the two-way nesting impact. We suggest that once the two-way nesting model provides a diabatic heating anomaly in the tropics, the climate system will be shifted along the leading dynamical mode inherent in the western North Pacific. In other words, the GCM bias correction by the INCL can be interpreted as the excitation of a near-neutral mode of the system by the INCL.

We would like to add some remarks on pioneering work by Lorenz and Jacob (2005) using a two-way nested GCM. First, looking at a zonal-mean temperature plot (not shown), we did not find any signals to relieve the temperature bias in the tropical mid-troposphere found in our GCM run (not shown). Second, despite their nesting domain being much smaller than ours, we presume that in their experiment the leading mode would come out in boreal summer. If so, the experiment could relieve the summer monsoon bias, although the difference of the basic state is expected to provide a difference in the leading mode. Extending the discussion in Neale and Slingo (2003), who suggested that diabatic heating attributed to sea-breeze circulation had a significant impact on the global climate in the context of a simple forcing-response problem, the inherent dynamical mode(s) should be emphasized not only for GCM bias correction, but also for understanding the role of the tropical western Pacific in the global climate. This paper showed only a single example in 1997 summer, but similar analyses with different years or with different seasons should be carried out for a deeper understanding of the dynamics in this region.

## Acknowledgments

We would like to thank two anonymous reviewers for providing many insightful comments that helped us to improve the manuscript. We also thank Drs. K. Saito, N. Ishizaki, I. Takayabu, and S. Hayashi for giving the first author many technical suggestions on the development of the INCL 3.0, and thank Profs. S.-P. Xie and Y. Wang for valuable discussions. We also thank Dr. Masahiro Watanabe for permission to use the linear baroclinic model. The JMA/MRI NHM embedded into the INCL system was used with the permission of the Japan Meteorological Agency. This study was mainly supported by Global Environment Research Fund S-5-3 of the Ministry of the Environment, Japan, partially supported by the Frontier Research Consortium on Climate and Environment Applications of the University of Tokyo with the Itochu Co., Nippon Telegraph and Telephone Co., and Tokyo Marine & Nichido Fire Insurance Co., Ltd., and partly supported by the Research Program on Climate Change Adaptation and by the Innovative Program of Climate Change Projection for the 21st Century (KAKUSHIN program) of the Ministry of Education, Culture, Sports, Science, and Technology (MEXT) of Japan. The first author was supported by the Research Program on Climate Change Adaptation and by Grants-in-Aid for Scientific Research on Innovative Areas 22106008 and for Young Scientists (B) 18740293 from MEXT. The model simulations were performed using the Hokkaido University High Performance Computing System. All figures were drawn using Grid Application Development Software (GrADS).

## References

Chen, W., Z. Jiang, L. Li, and P. Yiou, 2010: Simulation of regional climate change under the IPCC A2 scenario in southeast China. *Climate Dyn.*, **36**, 491–507.

Denis, B., R. Laprise, and D. Caya, 2003: Sensitivity of a regional climate model to the resolution of the lateral boundary conditions. *Climate Dyn.*, **20**, 107–126.

Hirota, N., and M. Takahashi, 2011: A tripolar pattern as an internal mode of the East Asian summer monsoon, in revision.

Hirota, N., M. Takahashi, N. Sato, and M. Kimoto, 2005: Change of the Baiu season climate in the East Asia during 1979 to 2003. *SOLA*, **1**, 137–140.

Hurrell, J. W., J. J. Hack, D. Shea, J. M. Caron, and J. Rosinski, 2008: A new sea surface temperature and sea ice boundary dataset for the community atmosphere mode. *J. Climate*, **21**, 5145–5153.

Inatsu, M., and M. Kimoto, 2009: A scale interaction study on East Asian cyclogenesis using a general circulation model coupled with an interactively nested regional model. *Mon. Wea. Rev.*, **137**, 2851–2868.

Ji, Y., and A. D. Vernekar, 1997: Simulation of the Asian summer monsoons of 1987 and 1988 with a regional model nested in a global GCM. *J. Climate*, **10**, 1965–1979.

Kimoto, M., 2005: Simulated change of the east Asian circulation under global warming scenario. *Geophys. Res. Lett.*, **32**, L16701.

Kosaka, Y., and H. Nakamura, 2006: Structure and dynamics of the summertime Pacific-Japan teleconnection pattern. *Quart. J. Roy. Meteor. Soc.*, **132**, 2009–2030.

Kosaka, Y., H. Nakamura, M. Watanabe, and M. Kimoto, 2009: Analysis on the dynamics of a wave-like teleconnection pattern along the summertime Asian jet based on a reanalysis dataset and climate model simulations. *J. Meteor. Soc. Japan*, **87**, 561–580.

Liebmann, B., and C. A. Smith, 1996: Description of a complete (interpolated) outgoing longwave radiation dataset. *Bull. Amer. Meteor. Soc.*, **77**, 1275–1277.

Lin, J.-L., K. M. Weickman, G. N. Kiladis, B. E. Mapes, S. D. Schubert, M. J. Suarez, J. T. Bacmeister, and M.-I. Lee, 2008: Subseasonal variability associated with Asian summer monsoon simulated by 14 IPCC AR4 coupled GCMs. *J. Climate*, **21**, 2008–2034.

Lorenz, P., and D. Jacob, 2005: Influence of regional scale information on the global circulation: A two-way nesting climate simulation. *Geophys. Res. Lett.*, **32**, L18706, doi: 10.1029/2005GL023351.

Navarra, A., 1993: A new set of orthonormal modes for linearized meteorological problems. *J. Atmos. Sci.*, **50**, 2569–2583.

Neale, R., and J. Slingo, 2003: The maritime continent and its role in the global climate: A GCM study. *J. Climate*, **16**, 834–848.

Nitta, T., 1987: Convective activities in the tropical western Pacific and their impact on the Northern-Hemisphere summer circulation. *J. Meteor. Soc. Japan*, **65**, 373–390.

North, G. R., T. L. Bell, R. F. Cahalan, and F. J. Moeing, 1982: Sampling errors in the estimation of empirical orthogonal functions. *Mon. Wea. Rev.*, **110**, 699–706.

Onogi, K., J. Tsutsui, H. Koide, M. Sakamoto, S. Kobayashi, H. Hatsushika, T. Matsumoto, N. Yamazaki, H. Kamahori, K. Takahashi, S. Kadokura, K. Wada, K. Kato, R. Oyama, T. Ose, N. Mannoji, and R. Taira, 2007: The JRA-25 reanalysis. *J. Meteor. Soc. Japan*, **85**, 369–432.

Saito, K., T. Fujita, Y. Yamada, J. Ishida, Y. Kumagai, K. Aranami, S. Ohmori, R. Nagasawa, S. Kumagai, C. Muroi, T. Kato, H. Eito, and Y. Yamazaki, 2006: The operational JMA nonhydrostatic mesoscale model. *Mon. Wea. Rev.*, **134**, 1266–1298.

Wang, B., R. Wu, and K.-M. Lau, 2001: Interannual variability of the Asian Summer monsoon: Contrasts between the Indian and the Western North Pacific-East Asian monsoons. *J. Climate*, **14**, 4073–4090.

Wang, B., R. Wu, and T. Li, 2003: Atmosphere-warm ocean interaction and its impact on Asian-Australian monsoon variation. *J. Climate*, **16**, 1195–1211.

Watanabe, M., and M. Kimoto, 2000: Atmosphere-ocean thermal coupling in the North Atlantic: A positive feedback. *Quart. J. Roy. Met. Soc.*, **126**, 3343–3369.

Xie, S.-P., K. Hu, J. Hafner, H. Tokinaga, Y. Du, G. Huang, and T. Sampe, 2009: Indian Ocean capacitor effect on Indo-Western Pacific climate during the summer following El Niño. *J. Climate*, **22**, 730–747.

Yasutomi, N., 2003: Detection and dynamics of principal modes of Asian summer monsoon variability, Department of Earth and Planetary Science, Graduate School of Science, The University of Tokyo, 100 pp.

Zwiers, F. W., 1993: Simulation of the Asian summer monsoon with the CCC GCM-1. *J. Climate*, **6**, 470–486.